A MODEL FOR PROPAGATION OF SHORT PULSES OF ULTRASOUND IN SOLID IMMERSED IN A FLUID

X. Jian[*], J. P. Weight[+], K.T. V. Grattan[+]
+City University, Department of Electrical, Electronic and Information Engineering, London EC1 0HB, UK
[*] Now at: University of Warwick, Department of Physics, Coventry CV4 7AL, UK
x.jian@warwick.ac.uk

Abstract

A novel model is developed to calculate field-point waveforms for a circular compression wave transducer water-coupled to a solid medium. The model makes use of known theory for propagation into a fluid medium and takes account of refraction and mode conversion at the fluid solid interface. Calculations made using the model are compared with experimental measurements of field-point waveforms made using a miniature piezoelectric receiving probe. The results obtained are relevant to immersion NDT.

I Introduction

Analytic solutions are available for the ultrasonic field radiated into a fluid medium ([1], for instance). In solids, were both longitudinal (compression) and transverse (shear) waves can propagate, the problem is more complicated and analytic solutions are generally not available. Exact numerical solutions using finite element and finite-difference[2] methods for the field in a solid have been given but are very time consuming. Other related work includes plane and edge wave models[3], approximate integral formulations[4], asymptotic methods[5] and the Cagniard method([6], for instance]). Here, we develop approximate integral formulations for the field in solids due to an angled, water-coupled transducer. An efficient method to evaluate the integral expressions is given. The results obtained are explained in terms of plane and edge waves.

II Theory

Figure 1 shows the model geometry. A Cartesian coordinate system is set with the origin at the centre of the source, the *XY* plane being parallel to a plane fluid/solid interface. Throughout, the angular alignment q_A of the source is such that its axis lies on the *XZ* plane. The piston source radiates compression waves into the fluid medium, to be refracted and mode converted at the fluid/solid interface. Consider the ray path of a wave radiating from a general source point X_0. The ray reaches field point X_s along a unique path $X_0X_IX_s$. where X_I is the point where the path crosses the interface. However such paths cannot be found analytically. X_0' and X_s' are the projections of points X_0 and X_s onto the interface. Path $X_0X_IX_s$ *and its projection* $X_0'X_IX_s'$ lie on the same plane, the plane being perpendicular to the interface. The line X_0X_s and the projection $X_0'X_s'$ intersect at X_I'. The incident angle q_I of each ray path and the angle of refraction q_R in the solid are related by Snell's Law.

Consider an idealised piston source undergoing impulsive motion and radiating into a fluid. The impulsive particle velocity potential at a general point X_f in the fluid from the vicinity s around the source point X_0 has been given by [1],

$$f_{d,s}(X_f,t;X_0,t_0)=\frac{c_f}{2p}\Omega_{d,s}(X_f,t;X_0,t_0) \qquad (1)$$

where c_f is the propagation velocity in fluid, t is the arrival time at a point X_f for a contribution leaving the source point X_0 at time t_0, and $\Omega_{d_s}(X_f,t;X_0,t_0)$ is the angle of equidistant arc subtended on the source surface at time t.

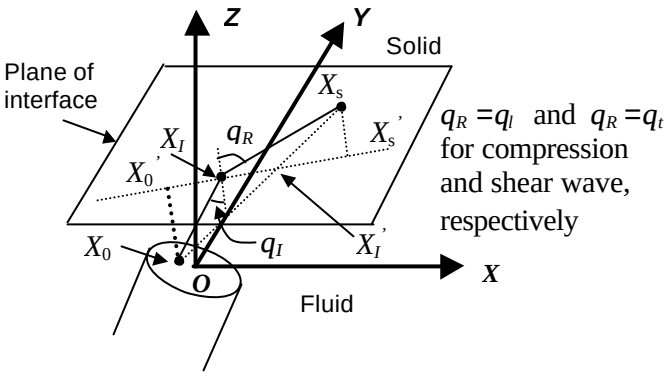

Figure 1: 3D Model geometry

Accordingly, the particle velocity is given by

$$u_{d,s}(X_f,t;X_0,t_0)=\frac{1}{c_f}\left(\frac{\partial f_{d,s}(X_f,t;X_0,t_0)}{\partial t}\right) \qquad (2)$$

The present model assumes that the incoming waves at the solid surface can be considered locally plane, the particle velocity within the solid becoming

$$u_{d,s,l}(X_s,t;X_0,t_0)=u_{d,s}(X_f,t;X_0,t_0)W_l(X_s,t;X_0,t_0) \qquad (3)$$

$$u_{d,s,t}(X_s,t;X_0,t_0)=u_{d,s}(X_f,t;X_0,t_0)W_t(X_s,t;X_0,t_0) \qquad (4)$$

where $W_l(X_s,t,X_0,t_0)$ and $W_t(X_s,t,X_0,t_0)$ are the refraction coefficients for compression and shear waves, respectively. Integrating over the whole source to give the impulse response and convolving this with the source velocity driving function $v(t)$, we express the compression particle velocity components as,

$$u_{l,x}(X_s,t)=v(t)*\frac{1}{2p}\frac{\partial}{\partial t}\int_S \sin q_l \cos a W_l(X_s,t;X_0,t_0)\Omega_{ds}(X_f,t;X_0,t_0)$$

$$u_{l,y}(X_s,t) = v(t) * \frac{1}{2p}\frac{\partial}{\partial t}\int_S \sin q_l \sin a\, W_l(X_s,t;\, X_0,t_0)\Omega_{ds}(X_f,t;\, X_0,t_0)$$

$$u_{l,z}(X_s,t) = v(t) * \frac{1}{2p}\frac{\partial}{\partial t}\int_S \cos q_l W_l(X_s,t\,;\, X_0,t_0)\Omega_{ds}(X_f,t;X_0,t_0) \quad (5)$$

Similarly for the shear wave, the particle velocity components are given by,

$$u_{t,z}(X_s,t) = v(t) * \frac{1}{2p}\frac{\partial}{\partial t}\int_S \sin q_t W_t(X_s,t;\, X_0,t_0)\Omega_{ds}(X_f,t;X_0,t_0)$$

$$u_{t,x}(X_s,t) = v(t) * \frac{1}{2p}\frac{\partial}{\partial t}\int_S \cos q_t \cos a\, W_t(X_s,t\,;\, X_0,t_0)\Omega_{ds}(X_f,t;\, X_0,t_0)$$

$$u_{t,y}(X_s,t) = v(t) * \frac{1}{2p}\frac{\partial}{\partial t}\int_S \cos q_t \sin a\, W_t(X_s,t;\, X_0,t_0)\Omega_{ds}(X_f,t;\, X_0,t_0) \quad (6)$$

III Numerical Calculation

The surface integrals within Eqns (5) and (6) cannot be solved explicitly. Here we give an efficient numerical evaluation that makes use of a coordinate transformation to divide the source into surface elements in a way that exploits symmetry and leads to a reduction in iteration times when calculating ray paths.

A Coordinate transformation

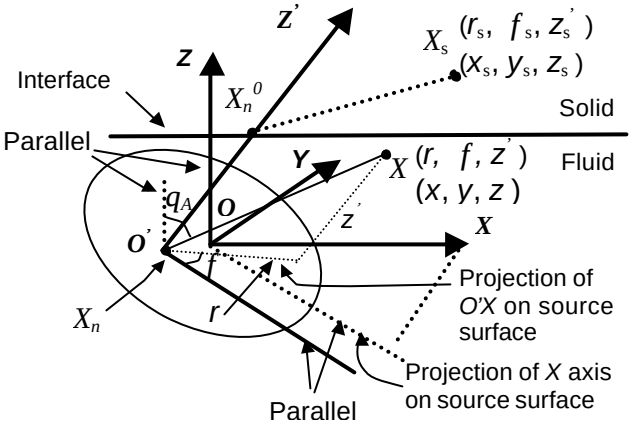

Figure 2: Coordinate transformation

Referring to Figure 2, we introduce a new cylindrical polar coordinates system (r, f, z'). The origin O' is set at points X_n that give the shortest travel time from the source surface to a given point X_s in the solid. Such minimum time paths must leave the source at normal incidence. Since X_n lies at different positions for the compression and shear waves, O' will shift accordingly. The Z' axis is perpendicular to the source surface and for $f = 0$, r lies in a direction parallel to the projection of OX on the source surface. Transformations from the Cartesian system $0XYZ$ are given by,

$$\begin{bmatrix} x \\ y \\ z \end{bmatrix} = \begin{bmatrix} \cos q_A & 0 & \sin q_A \\ 0 & 0 & 1 \\ -\sin q_A & 0 & \cos q_A \end{bmatrix} \begin{bmatrix} r_0 \cos f_0 + r\cos f \\ r_0 \sin f_0 + r \sin f \\ z_0' \end{bmatrix} \quad (10)$$

where (r_0, f_0, z_0') are the cylindrical coordinates of the source centre.

B Source surface elements

A general source element is shown in Figure 3 represented by a point of coordinate (r_i, f_j, z') where $z' = 0$. The element is bounded by arcs $r = r_i + Dr/2$ and $r = r_i - Dr/2$, and radius $f = f_j - Df/2$ and $f = f_j - Df/2$. The source elements are incremented as,

$$r_i = i\Delta r,\ \Delta r = c_f \Delta t,\ i = 1,\cdots, N_r(f_j)$$

$$f_j = j\Delta f,\ \Delta f = 2p / N_j,\ j = 1,\cdots, N_f \quad (11)$$

where Δt is a time step, and $N_r(f_j) = r_{rim}(f_j)/\Delta r$, $r_{rim}(f_j)$ being the distance from O' to the source rim at angle division f_j In the current work sufficient accuracy was obtained by setting $N_\phi = 180$.

Note that there is symmetry to the plane $f = 0$ for the contribution from each element of the source, for example pairs A and A'. This leads to a reduction in overall calculation times. For example, when X_n lies on the source diameter, the number of calculations is halved.

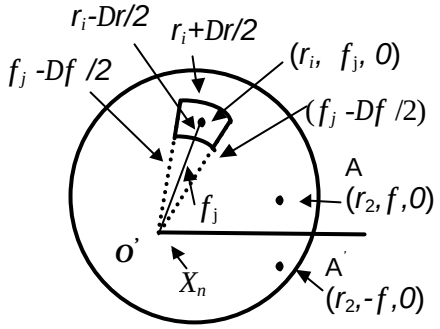

Figure 3: Symmetry in the polar coordinate system

C Propagating path

Considering the ray path from source element $(r_i, f_j, 0)$ in Figure 3, X_I must lie between point X_0' and X_s, but its position cannot be found analytically. Here, we iterate towards a sufficiently accurate solution. We first set $X_{i,j}^1 = X_0'$ and $X_{i,j}^2 = X_I'$. Set either $X_{i,j}^0 = X_n^0$, if $i = 0$ and X_n^0 is between X_I' and X_0', or set $X_{i,j}^0 = X_{i-1,j}^0$ where $X_{i-1,j}^0$ is approximation of X_I for source element $(r_{i-1}, f_j, 0)$, if $X_{i-1,j}^0$ is between X_I' and X_0'. The error at the current iteration is given by

$$Err = \frac{c_s}{c_f}\frac{\left|X_{i,j}^0 - X_{i,j}^1\right|}{\left|X_{i,j}^0 - X_0\right|} - \frac{\left|X_{i,j}^0 - X_{i,j}^2\right|}{\left|X_{i,j}^0 - X_s\right|}$$ where c_s is the propagation velocity for either the compression or the shear wave in the solid. If Err is -tve, $X_{i,j}^1 = X_{i,j}^0$, if

Err is +tve, $X^{2}_{i,j} = X^{0}_{i,j}$. Set $X^{0}_{i,j} = X^{1}_{i,j} + X^{2}_{i,j}$ again and continue until $Err \le 0.01$, then $X_I \approx X^{0}_{i,j}$.

D Numerical integral procedure

When calculating the impulse response, we increment time according to $t_k = t_0 + (k-1)\Delta t$, $k = 1, \cdots, N_t$, $N_t = t^s_{\max} / \Delta t$, where $t^s_{\max}$ is the maximum travel time from source rim to X_s. It was found that a time increment of 10 ns gave a good compromise between accuracy and calculation times. Using the propagation path as found in section C above and equations (11), (3) and (4), the compression and shear contribution of each source element is calculated. Summation according to (5) and (6), and repeating for each time step gives the overall impulse response at a given point in the solid.

Note that, of itself, the origin shift in the coordinate transformation of **A** above leads to a reduction in calculation times by ensuring that each element in the surface integral contributes to the impulse response in time sequence.

IV Results

A Measurement set up

The measurement set up is shown in Figure 4 and is discussed in greater detail elsewhere[7]. A single disc-shaped test piece was used for all of the results given here. The test piece was constructed from mild steel with density $r = 7800\ kgm^{-3}$, and compression and shear wave velocity $5960 ms^{-1}$ and $3210 ms^{-1}$, respectively.

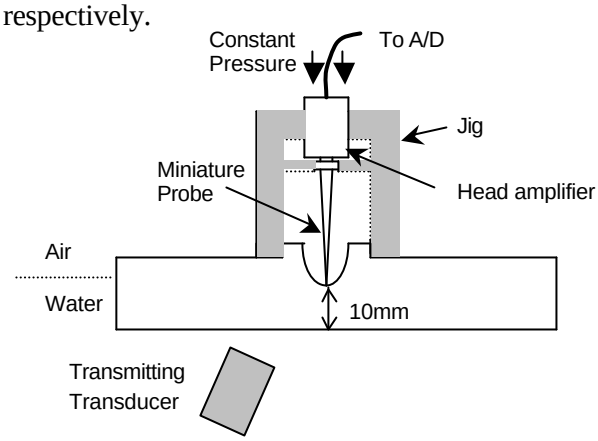

Figure 4: Measurement set up

The waveforms at the surface of the test piece were measured with the miniature probe supported by a specially constructed jig to avoid any variation in coupling conditions. It has been shown that to a reasonable approximation, such a probe measures the normal component of particle velocity in a solid [7].

The transmitter was a wideband Panametrics transducer of diameter 19mm, that gave a short pulse approximating to 1 cycle at 2MHz. Its orientation to the solid surface and its position in 3 axes could be adjusted.

B Normal incidence

Figure 5 shows measured and calculated results made using the new model for axial field-point waveforms in steel (metal path 10mm) with the transmitting transducer normally coupled at various water paths. The results are shown to the same time scale, but a different arbitrary, time origin is used for each result. The first pulse to arrive labelled PC is due to reception of the "plane compression" wave[3] from the transducer. The time differences between PC and the pulses labelled EC ("edge compression"[3]) are consistent with the reception of a wave from the rim of the source, allowing for refraction and taking the compression wave velocities in the fluid and solid. Similarly, the arrival times of the ES ("edge shear") pulses are consistent with reception of waves from the source rim that propagate at the compression wave velocity in the fluid and the shear-wave velocity in the solid. As in earlier work[3], the origin of the shear edge wave is explained as a result of partial mode conversion of the compression edge wave. Since the refraction angles decrease as the coupling path increases, such mode conversion will also decrease with coupling path, an effect that can be seen in the results of Figure 5.

In general there is good agreement between the measured and calculated results, justifying the assumptions made in developing the model.

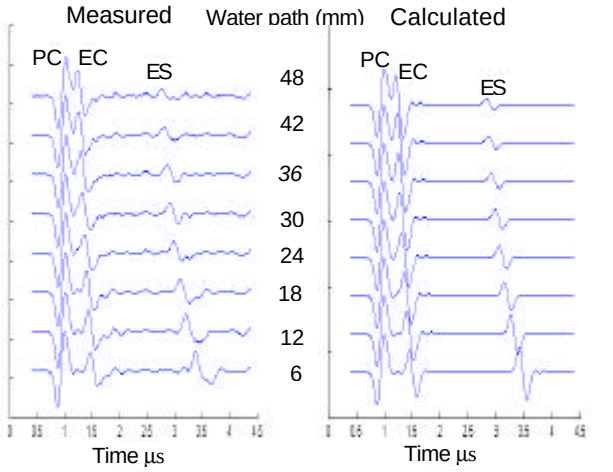

Figure 5: Field-point waveforms in steel using various water paths. Incident angle: normal.

C Oblique incidence

As can be seen in the results of Figure 6, at oblique incidence the incident compression plane wave can partially mode convert to give a shear plane wave in the solid. According to the present model, for oblique incidence at less than the 1st critical angle, the field in a solid has four components: a compression plane (PC) and edge wave (EC) and a shear plane (PS) and edge wave(ES).

The results given in Figure 6 are for four positions of the transmitting transducer along the *X* axis (see Figure 1). Position (*a*) gives a maximum amplitude for the compression edge wave as received by the miniature probe: similarly (*d*) gives a maximum for the shear edge wave. We define these positions as the "focus" for each edge wave. Since at oblique incidence we have an elliptic beam in the solid, the foci do not in general correspond with the axes of the corresponding plane wave beams – unlike the situation at normal incidence, where as a result of circular symmetry, the edge wave pulses are maximum on the *axis*. At the focus of the compression edge wave (a), the shear plane wave is smaller than in (d) since in (a) the shear plane wave beam is just beginning to "miss" the receiving probe. Results (b) and (c) show the plane- and edge-wave components at positions in between the two foci.

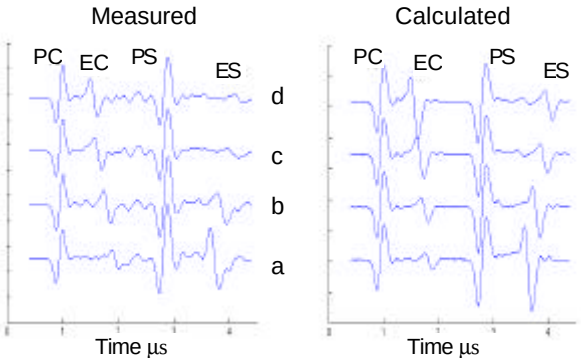

Figure 6: Field-point waveforms at the same range in steel but at different field-point positions. Water path: 6mm; incident angle: 12^{o} .

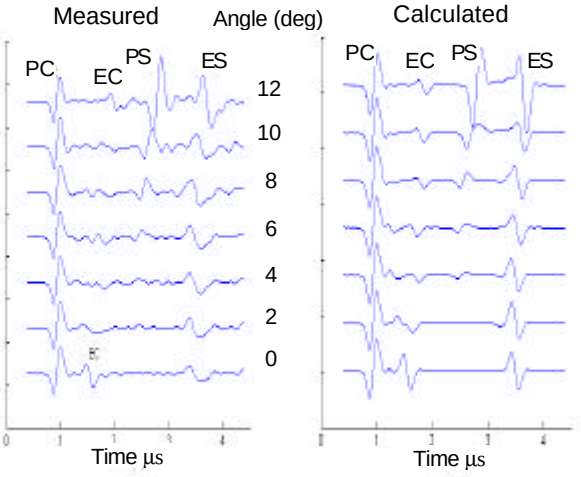

Figure 7: Field-point waveforms at various angles of incidence. Water path: 6mm (from centre of transducer).

Figure 7 shows how the field-point waveforms change with incident angle from 0^{o} to 12^{o}. In each case, the measurements were made at the focus of the shear edge wave. As we would anticipate from well-known refraction coefficients, we see an increase in amplitude of the shear plane wave with incident angle. The change in amplitude with angle of the ("focussed") shear-edge wave pulse is due to a combination of refraction and the directivity of the incident compression edge wave.

V Conclusion

Experimental measurements of field-point waveforms in steel show that the field radiated into a solid by a water-coupled, compression-wave transducer can be explained in terms of four main components: compression plane- and edge-waves, and shear plane- and edge-waves. The measurements were made at the steel surface using a miniature piezoelectric probe that approximately responds to the normal component of particle velocity.

Corresponding numerical calculations - made using a model that assumes the rays from each element of the source are refracted and mode converted according to well-known refraction coefficients for plane waves - agree well the measurements. The model makes use of coordinate transformations to exploit symmetry and reduce calculation times.

The plane and edge-wave description of the pulsed field is useful in describing the complicated structure of the field in solids. Note that even at incident angles between the 1^{st} and 2^{nd} critical angles, where only shear waves exist in the solid, the field still has a plane- and edge-wave structure.

Acknowledgements

The authors are grateful to Professor Fradkin L. J., South Bank University for her helpful advice and to the ESPRC for financial support.

References

[1] A. Ilan and J.P.Weight, "The propagation of short pulses of ultrasound from a circular source coupled to an isotropic solid", *JASA, vol. 88*, pp.1142-1151, 1990.

[2] P.R. Stepanishen and G. Fisher., "Experimental verification of the impulse response method to evaluate transient acoustic fields", *JASA, vol. 69*, pp. 1610-1617, 1981.

[3] J.P. Weight, "A model for the propagation of ultrasonic pulses in a solid medium", *JASA, vol. 81*, pp. 815-827, 1987.

[4] A. Lhemery, "A model for the transient ultrasonic field radiated by an arbitrary loading in a solid", *JASA, vol 96*, pp. 3776-3786, 1994.

[5] D. Gridin and L. J Fradkin., "The high-frequency asymptotic description of pulses radiated by a circular normal transducer into an elastic half-space," *JASA* 104, 3190-3198, 1998.

[6] M. C. Bakker and M. D. Verweij, "Experimental validation of two elastodynamic models for the wave field generated by an ultrasonic transducer," *JASA vol 113*, pp. 1850-1862, 2003.

[7] X. Jian , J. P. Weight and K. T. V., Grattan "Characterisation of a miniature wide-band ultrasonic probe to measure compression and shear waves in solid media". In proceedings of the *5th WCU, Paris*, 2003.